

Optimal Throughput and Energy Efficiency for Wireless Sensor Networks: Multiple Access and Multi-packet Reception

Wenjun Li and Huaiyu Dai

Abstract

We investigate two important aspects in sensor network design—the throughput and the energy efficiency. We consider the uplink reachback problem where the receiver is equipped with multiple antennas and linear multiuser detectors. We first assume Rayleigh flat fading, and analyze two MAC schemes: round-robin and slotted ALOHA. We optimize the average number of transmissions per slot and the transmission power for two purposes: maximizing the throughput, or minimizing the effective energy (defined as the average energy consumption per successfully received packet) subject to a throughput constraint. For each MAC scheme with a given linear detector, we derive the maximum asymptotic throughput as the signal-to-noise ratio goes to infinity. It is shown that the minimum effective energy grows rapidly as the throughput constraint approaches the maximum asymptotic throughput. By comparing the optimal performance of different MAC schemes equipped with different detectors, we draw important tradeoffs involved in the sensor network design. Finally, we show that multiuser scheduling greatly enhances system performance in a shadow fading environment.

Index Terms

Throughput, Energy Efficiency, Multiuser Diversity, Scheduling, Slotted ALOHA, Linear Multiuser Detector

Department of Electrical and Computer Engineering, North Carolina State University, Raleigh, NC 27606. (email: wli5, huaiyu_dai@ncsu.edu)

I. INTRODUCTION

Wireless sensor networks have become one of the burgeoning research fields in recent years, as they are envisioned to have wide applications in military, environmental, and many other fields [1]. Since sensors typically operate on batteries, of which replenishment is often difficult, a lot of work has been done to minimize the energy expenditure and prolong the sensor lifetime through energy efficient designs across layers [2]–[6]. Meanwhile, the sensor network should be able to maintain a certain throughput, (which is equivalent to a certain delay constraint), in order to fulfill the QoS requirement of the end user, and to ensure the stability of the network. Typically, the throughput and the energy efficiency are inconsistent, and there exists a tradeoff between the two measures. The objective of this work is to explore the maximum achievable throughput under certain network configurations and receiver structures, as well as optimal network designs that achieve the desired throughput with minimal energy consumption.

We consider the reachback problem where all sensor nodes in the sensor field transmit to a common receiver. The receiver has replenishable power supply and possesses sophisticated data reception and processing capabilities. An alternative way for transmitting data, typically in a non-hierarchical sensor network, is the multi-hop communication, whereby a packet is received and forwarded by intermediate nodes several times before reaching the destination. While multi-hop communication may lower the transmission energy by mitigating the exponential decay in the signal power as a function of the distance, this energy saving can hardly justify the extra energy spent on packet reception, processing, routing and forwarding. Moreover, multi-hop communication also incurs more contentions/interference and delays, as indicated in [7], [8]. As exemplified by the Sensor Networks with Mobile Agents (SENMA) [9], employing a powerful receiver, such as a mobile agent, conserves sensors' energy by freeing them from packet relaying, routing and data processing routines, and good performance can be guaranteed even with minimal transmission power.

We assume that each node constantly has packets to transmit; the transmission is slotted and the slot length T equals the transmission time of one packet. The sensors and the receiver constitute a multiple access network. Under the traditional collision channel model (i.e., single transmission means success and simultaneous transmissions results in failure), the throughput of the multiple access network is limited: the maximum throughput per slot is 1 for time-division-multiple-access

(TDMA), and is only $1/e$ for slotted ALOHA with optimal decentralized control [10]. Such a throughput may not be sufficient for sensor network applications. Nevertheless, advanced signal processing techniques such as multiuser detection [11] enable correct reception of simultaneous transmitted packets at the physical layer, and consequently, Ghez *et. al.* proposed the multi-packet reception model [12], which revolutionized the underlying assumption of MAC layer design. In this work we assume that the receiver is equipped with N antennas and a linear multiuser detector followed by single-user decoders. The packet transmission is considered successful as long as the output signal-to-interference-ratio (SIR) of the linear detector is above a certain threshold β [13]. The transmitting sensors and the receive antenna array thus form a virtual multiple-input-multiple-output (MIMO) system, which can also be viewed as a space-division multiple access (SDMA) system. Note that due to the analogy between the direct-sequence code-division multiple access (DS-CDMA) system and the MIMO system, the analysis in this paper can also be adapted to the DS-CDMA system with a single receive antenna and spreading gain N . But since the received power adds up across the antennas, the MIMO system requires only $1/N$ of the transmission power of the corresponding DS-CDMA system. A hybrid of CDMA and multiple receive antenna system is also possible, in which case the performance is further enhanced by the effect of “resource-pooling” [14].

A sensor field usually consists of hundreds or thousands of sensors, and the number of transmissions in each slot at the same frequency band is typically much smaller to avoid the excessive multiple access interference. Therefore, in addition to the SDMA that defines the channelization in each slot, another level of medium access control is necessary to determine which sensors should transmit during each slot, and the MAC scheme for this purpose can be either coordinated or random. For coordinated access, we consider round-robin, which is TDMA in essence: the adjacent sensors form a transmission group and the groups are scheduled for access one by one. For random access, we consider the simplest form of slotted ALOHA, known as Delayed First Transmission (DFT) [15]: in each slot every sensor node transmits a packet (new or retransmission) with the same probability p independently. We assume that the receiver transmits a beacon at the beginning of each slot for synchronization [9], [16]. It might require some overhead for the sensor nodes to get some delay estimates for synchronization purpose, and then they can adjust their timing when simultaneously transmitting. It is known that slotted ALOHA is simple and is preferred when the traffic is bursty, but it suffers from

certain performance degradation from centrally-controlled networks, and we will investigate the exact performance loss in our system. In addition to different MAC schemes, the linear multiuser detector at the receiver can be the single-user matched filter, the decorrelating detector, or the linear MMSE detector. As we will see, both the MAC scheme and receiver structure employed have significant impact on the system performance. For a given MAC scheme with a given linear detector, we optimize the transmit power, as well as the transmission group size (for round-robin) or the transmission probability (for slotted-ALOHA). We study two optimization problems: one is to maximize the throughput, and the other is to minimize the energy consumption subject to a throughput constraint.

We then modify our assumption of pure Rayleigh-fading by admitting shadow fading into our system model. Multiuser diversity can be realized in such a system by allowing the sensor group with the best shadowing coefficient to transmit during each slot, and is shown to have great significance in energy-conservation for sensor networks. Fairness concerns of multiuser scheduling can be remedied by enabling the movement of the receiver to induce a dynamic shadowing environment, or other known algorithms with little throughput sacrifice (see Section VI).

Most related papers on the performance and optimal resource allocation of multiple access networks are based on the collision model. The optimization of transmission probability for slotted ALOHA scheme with or without uplink CSI are studied in [17]–[19]. Relatively few works in this direction adopted the multi-packet reception model [16], [20]. The design of transmission probability of slotted ALOHA scheme by exploiting uplink CSI in a distributed fashion is studied in [16]. In [20], the authors analyze slotted-ALOHA sensor networks with multiple mobile agents, whose covering areas can be optimally designed to maximize the throughput or to maximize the energy efficiency. The performance analysis of sensor networks using both CDMA and multiple receive antennas is presented in [21] based on the results on large random networks in [14]. The analysis in this paper does not rely on the large network approximation. Meanwhile, most studies on multiuser scheduling for uplink or downlink wireless networks have focused on maximizing the information-theoretic capacity [22]–[25]. In [26], the authors present a scheduling algorithm which maximizes a certain performance value estimated by the user or calculated by the base station, such as a linear function of the SINR. On the other hand, we study multiuser scheduling by assuming the MPR model due to suboptimal receivers, where the main performance measure

is the throughput in terms of the average number of successful packets per slot.

The main contribution of this work is as follows:

- 1) We derive the throughput and the effective energy (average energy consumption for each successful packet) for multiple access network employing round-robin and slotted ALOHA in Rayleigh flat fading.
- 2) We optimize the transmission power and the average number of transmissions per slot to
 - a) Maximize the throughput: For each MAC scheme with a linear detector, we derive the maximum asymptotic throughput when the signal-to-noise ratio goes to infinity.
 - b) Minimize the effective energy subject to a throughput constraint: It is shown that the minimum effective energy grows rapidly as the throughput constraint approaches the maximum asymptotic throughput.
- 3) By comparing the optimal performance of different MAC schemes equipped with different detectors, we draw important tradeoffs involved in the sensor network design.
- 4) We show that multiuser scheduling can significantly enhance the system performance in a shadow fading environment.

The organization of the paper is as follows. In Section II, we introduce the system model, some assumptions of our work, and the general measures of the throughput and the energy efficiency. In Section III, we briefly describe the three linear detectors of interest and derive the analytical results to be used later. In Section IV, we first derive the energy efficiency and the throughput of the round-robin and slotted ALOHA scheme, and then study the two optimization problems, throughput maximization and throughput-constrained energy minimization respectively. Numerical results and discussions are presented in Section V. Section VI studies multiuser scheduling in the shadow fading environment. Section VII contains the concluding remarks.

II. SYSTEM DESCRIPTION

We assume that there are totally n sensors in the sensor field, the receiver is equipped with N antennas, and the SIR threshold is β . The diameter of the sensor field is much smaller than the distance between the sensor field and the receiver, and there exists a rich-scattering environment between the sensor field and the receiver, e.g., the sensors are deployed in a building or a forest. Therefore the channel states between each sensor and each receive antenna can be modeled as independent, identical Rayleigh variables. We assume that sensors have no knowledge of uplink

channel state information (CSI), and transmit with equal power P . If m sensors simultaneously transmit, the m sensors and N receive antennas form a virtual MIMO system, and the discrete-time model is given by

$$\mathbf{y} = \sqrt{G} \sum_{i=1}^m \mathbf{h}_i x_i + \mathbf{n}, \quad (1)$$

where x_i is the transmitted signal of the i -th sensor and $E[|x_i|^2] = P$, \mathbf{h}_i is the $N \times 1$ spatial signature of the i -th sensor, whose entries are independent circularly-symmetric complex Gaussian variables with zero mean and unit variance, G is the common pathloss, \mathbf{n} is the noise vector with zero mean circularly-symmetric complex Gaussian entries and covariance matrix $\sigma^2 \mathbf{I}$, and \mathbf{y} is the received signal vector. The average received SNR of a packet at one receive antenna is given by $\rho = \frac{PG}{\sigma^2}$. In the following we denote the matrix $\mathbf{H} = [\mathbf{h}_1, \mathbf{h}_2, \dots, \mathbf{h}_m]$.

We assume that a feedback channel exists from the receiver to the sensor nodes, which is used for synchronization, acknowledgements, group selection and other signaling on the MAC layer. The bandwidth of the feedback channel is typically small and thus the energy consumption for receiving the signaling is assumed to be negligible throughout the paper. For simplicity, we also ignore the circuit energy consumption, which can be incorporated and the optimizations described in this paper can be performed with minor modifications. Some measures of sensor network's energy efficiency have been explored in the literature: In [5], the *energy consumption per bit* to achieve a desired bit-error-rate is evaluated, and in [20], the metric *efficiency*, defined as the average number of successes over the total number of transmissions, is studied for SENMA networks. The former metric does not assume a multi-packet reception model, and the latter does not characterize the exact energy expenditure, as a transmission scheme with high efficiency is not necessarily energy efficient if the transmit power is not constrained. We combine the ideas in these two papers and measure the energy efficiency by the *effective energy* [21], defined as the average energy consumption per successfully transmitted packet:

$$E_e = \frac{PT}{\Pr[\text{succ}]}, \quad (2)$$

where $\Pr[\text{succ}]$ is the average probability of success for a transmitted packet. Note that the effective energy directly determines the number of packets a sensor can successfully transmit during its life time. The *throughput*, denoted by λ , is defined as the average number of successful

transmissions per slot. Denote a as the average number of transmissions per slot, we have

$$\Pr[\text{succ}] = \frac{\lambda}{a}. \quad (3)$$

Throughout the work we assume that the number of receive antennas N , the total number of sensors n , the SIR threshold β , the common pathloss G , as well as the noise variance σ^2 are fixed. When G and σ^2 are fixed, the optimization of the transmission power P is the same as the optimization of ρ .

III. LINEAR MULTIUSER DETECTORS IN RAYLEIGH FADING CHANNELS

Assume that m sensors simultaneously transmit and the SNR is ρ , then the outcome of the i th transmitted packet (success is denoted by 1 and failure is denoted by 0) is a random variable determined by the channel realization:

$$o_i(\mathbf{H}) = \mathcal{I}(\text{SIR}_i \geq \beta | m, \rho, \mathbf{H}), \quad (4)$$

where $\mathcal{I}(\cdot)$ denotes the indicator function. The expected value of the outcome averaged over all channel realizations is denoted by $q(m, \rho)$, which is the same for all i :

$$q(m, \rho) = E_{\mathbf{H}}[o_i(\mathbf{H})] = \Pr[\text{SIR}_i \geq \beta | m, \rho]. \quad (5)$$

In an ergodic channel, the average number of successes when there are m transmissions per slot and SNR is ρ is given by

$$E_{\mathbf{H}} \left[\sum_{i=1}^m o_i(\mathbf{H}) \right] = \sum_{i=1}^m E_{\mathbf{H}}[o_i(\mathbf{H})] = mq(m, \rho). \quad (6)$$

As we will see, the throughput and the effective energy for round-robin and slotted-ALOHA are functions of $q(m, \rho)$, which is determined by the physical channel and the linear detector used. In general $q(m, \rho)$ decreases with m and increases with ρ . In this section, we briefly describe the three linear detectors of interest, and derive the expression of $q(m, \rho)$ in Rayleigh fading channels for each detector. Moreover, as we will use the asymptotic value of $q(m, \rho)$ as $\rho \rightarrow \infty$ frequently in later analysis, we also derive the expression of $q(m, \infty) \doteq \lim_{\rho \rightarrow \infty} q(m, \rho)$. The readers are referred to [11] for more details of these multiuser detectors.

A. Matched Filter

The matched filter only requires the knowledge of the spatial signature of the desired user, which is suitable for the downlink but not much of an advantage for the uplink where the knowledge of spatial signatures of all users are known. The SIR of the i -th user after matched-filtering is given by

$$\text{SIR}_i = \frac{PG\|\mathbf{h}_i\|^4}{\sigma^2\|\mathbf{h}_i\|^2 + PG\sum_{j=1, j \neq i}^m \|\mathbf{h}_i^\dagger \mathbf{h}_j\|^2}, \quad (7)$$

where \dagger denotes conjugate transpose.

Lemma 3.1: The $q(m, \rho)$ of the matched filter in the Rayleigh fading channel is given by

$$q^{\text{mf}}(m, \rho) = \begin{cases} 1 - \Gamma(\beta/\rho, N), & m = 1, \\ \frac{1}{(m-2)!} \int_0^\infty [1 - \Gamma(\beta y + \beta/\rho), N] y^{m-2} e^{-y} dy, & m > 1. \end{cases} \quad (8)$$

where $\Gamma(a, x)$ is the regularized gamma function given by $\Gamma(a, x) = \frac{\int_0^x t^{a-1} e^{-t} dt}{\int_0^\infty t^{a-1} e^{-t} dt}$.

In the case $\rho \rightarrow \infty$,

$$q^{\text{mf}}(m, \infty) = \begin{cases} 1, & m = 1, \\ 1 - I\left(\frac{\beta}{1+\beta}; N, m-1\right), & m > 1, \end{cases} \quad (9)$$

where $I(x; a, b)$ is the regularized beta function, given by $I(x; a, b) = \frac{\int_0^x t^{a-1} (1-t)^{b-1} dt}{\int_0^1 t^{a-1} (1-t)^{b-1} dt}$.

Proof: See Appendix I.

B. Decorrelating Detector

The decorrelating detector is optimal according to three different criteria: least squares, near-far resistance, and maximum-likelihood when the received amplitudes are unknown [11]. When the spatial signatures are independent, the decorrelator exhibits improved performance than the matched filter except at low signal-to-noise ratios, and it converges to the linear MMSE detector at high signal-to-noise ratios. Generally, the decorrelator allows simpler expressions as it decomposes a multiuser channel into parallel single-user Gaussian channels. If $\mathbf{H}^\dagger \mathbf{H}$ is invertible, the SIR of the i -th user using a decorrelating detector is given by

$$\text{SIR}_i = \frac{\rho}{\left[(\mathbf{H}^\dagger \mathbf{H})^{-1} \right]_{ii}}, \quad (10)$$

and when $\mathbf{H}^\dagger \mathbf{H}$ is singular, SIR_i is zero.

Lemma 3.2: The $q(m, \rho)$ of the decorrelator in the Rayleigh fading channel is given by (c.f. (8) for the definition of the $\Gamma(a, x)$ function),

$$q^{\text{dec}}(m, \rho) = \begin{cases} 1 - \Gamma(\beta/\rho, N - m + 1), & m \leq N, \\ 0, & m > N. \end{cases} \quad (11)$$

When $\rho \rightarrow \infty$,

$$q^{\text{dec}}(m, \infty) = \begin{cases} 1, & m \leq N, \\ 0, & m > N. \end{cases} \quad (12)$$

Proof: See Appendix II.

C. Linear MMSE Detector

The linear MMSE detector cancels the interference and noise in an optimal way, such that the mean squared error is minimized among linear detectors. It can be shown that the linear MMSE detector also maximizes the SIR [11], hence it is optimal among linear detectors under the multiple packet reception model where the success probability only depends on the SIR. For the linear MMSE receiver, it can be shown that the SIR of the i -th user is given by

$$\text{SIR}_i = \mathbf{h}_i^\dagger \left(\mathbf{H}_i \mathbf{H}_i^\dagger + \frac{1}{\rho} \mathbf{I} \right)^{-1} \mathbf{h}_i, \quad (13)$$

where \mathbf{H}_i denotes the matrix obtained by striking out the i -th column of \mathbf{H} . There is no straightforward closed-form expression of $q(m, \rho)$ for the linear MMSE detector in the Rayleigh fading channel. An approximation of $q^{\text{mmse}}(m, \rho)$ can be obtained by using recent results on linear multiuser detectors in large random networks [27], where the SIR is shown to approach a Gaussian distribution as N approaches infinity, with $\alpha = m/N$ fixed. However, simulations show that such approximations are not accurate enough when N is relatively small, so in this paper we use exact success probabilities obtained through simulations for the linear MMSE detector. Nevertheless, when $\rho \rightarrow \infty$, the success probability of the linear MMSE detector has a simple form, given by the following lemma.

Lemma 3.3: For Rayleigh fading channels (c.f. (9) for the definition of the $I(x; a, b)$ function),

$$q^{\text{mmse}}(m, \infty) = \begin{cases} 1, & m \leq N, \\ 1 - I\left(\frac{\beta}{1+\beta}; N, m - N\right), & m > N. \end{cases} \quad (14)$$

Proof: See Appendix III.

IV. THROUGHPUT AND ENERGY OPTIMIZATIONS

In this section, we first derive the general expressions of the throughput and the effective energy for the round-robin and slotted ALOHA schemes, and then study the two optimization problems, throughput maximization and throughput-constrained energy-minimization for both MAC schemes.

A. Throughput and Effective Energy of Round-Robin and Slotted ALOHA

1) *Round-robin*: Round-robin is a fair scheduling scheme and is relatively easy to implement: m sensors in close proximity form a group. For simplicity we assume that n is a multiple of m , so there are totally $K = n/m$ groups. Groups are scheduled for access one by one, and when a group is scheduled in a slot, all the sensors in that group transmit simultaneously. It is easily seen that in an ergodic fading channel (shown at the beginning of Section III), the throughput of round-robin is

$$\lambda_{\text{rr}}(m, \rho) = mq(m, \rho). \quad (15)$$

With $P = \rho\sigma^2/G$, the effective energy of round-robin is given by

$$E_{\text{e,rr}}(m, \rho) = \frac{\rho\sigma^2 T/G}{q(m, \rho)}. \quad (16)$$

2) *Slotted ALOHA*: To employ the decorrelating detector or the linear MMSE detector in a slotted ALOHA system requires that the receiver knows the number and the channels of the transmitting nodes. For example, the sensors can signal their intention of transmission in a short reservation period at the beginning of each slot. We consider the type of slotted ALOHA where the transmission probability for all packets (new or retransmissions) is the same. Denoting the transmission probability of each user by p , the throughput of slotted ALOHA is given by

$$\lambda_{\text{sa}} = \sum_{k=1}^n \binom{n}{k} p^k (1-p)^{n-k} kq(k, \rho). \quad (17)$$

The average number of transmissions per slot is $a = np$. In the case n is large and p is small, we can approximate the binomial probabilities with Poisson probabilities and obtain

$$\lambda_{\text{sa}}(a, \rho) = e^{-a} \sum_{k=1}^n \frac{a^k}{k!} kq(k, \rho) = e^{-a} \sum_{k=1}^n \frac{a^k}{(k-1)!} q(k, \rho). \quad (18)$$

The average success probability is $\Pr[\text{succ}] = \lambda_{\text{sa}}(a, \rho)/a$, thus the effective energy is given by

$$E_{e,\text{sa}}(a, \rho) = \frac{\rho\sigma^2 T/G}{\lambda_{\text{sa}}(a, \rho)/a}. \quad (19)$$

The receiver can simply inform the sensors of the transmission probability, or the sensors can compute the optimum transmission probability if they have the knowledge of n . Slotted ALOHA also has built-in fairness, since the transmission probability is independent of the channel states of individual sensors.

B. Throughput Maximization

As we have shown, the throughput depends on both the MAC scheme as well as the type of the linear detector used. For a given MAC scheme with a given linear detector, the throughput is a function of the SNR ρ and the average number of transmissions per slot a (for round-robin, $a = m$, and for slotted ALOHA, $a = np$). These parameters can be chosen judiciously such that the throughput is maximized. The performance of various MAC schemes with different linear detectors can then be compared, in terms of the maximum throughput. In the following we focus on the joint optimization of a and ρ ; the optimization of a single parameter is straightforward and is therefore omitted.

First assume that a is fixed. Since $\Pr[\text{succ}]$ increases with ρ , the maximum throughput for any fixed a is achieved when $\rho \rightarrow \infty$. Therefore the maximum throughput jointly optimized over a and ρ is obtained by letting $\rho \rightarrow \infty$, and searching for the optimal a that achieves the global maximum. In practical systems, the sensors' power amplifier has a maximum output limit [5], which in turn poses an upper limit on ρ , denoted by ρ_{max} . Then the maximum throughput is achieved at ρ_{max} , and the problem again reduces to a single-parameter optimization problem. Nevertheless, the maximum throughput with no power constraint ($\rho \rightarrow \infty$) is of special interest as it represents the upper bound on the throughput that can be achieved by a MAC scheme with a given type of linear detector. In the following we discuss this case in detail.

For a given MAC scheme with a given linear detector, we define the *maximum asymptotic throughput* as the maximum throughput achievable with a given number of receive antennas as SNR ρ approaches infinity, and denote it by $\Lambda(\infty) \doteq \max_a \lambda(a, \infty)$. The maximum asymptotic throughput plays an important role in throughput-constrained energy minimization to be discussed

in Section IV.C, in the sense that any throughput constraint larger than $\Lambda(\infty)$ can not be attained. With a general linear detector, we have the following proposition:

Proposition 4.1: The maximum asymptotic throughput of round-robin and slotted ALOHA are respectively given by

$$\Lambda_{\text{rr}}(\infty) = \max_m mq(m, \infty); \quad (20)$$

$$\Lambda_{\text{sa}}(\infty) = \max_a e^{-a} \sum_{k=1}^n \frac{a^k}{(k-1)!} q(k, \infty), \quad (21)$$

The above expressions can be evaluated for different detectors using (9), (12) and (14).

Remark 1: With the decorrelating detector, the maximum asymptotic throughput of the two MAC schemes are respectively given by

$$\Lambda_{\text{rr}}^{\text{dec}}(\infty) = N, \quad \text{with } m = N; \quad (22)$$

$$\Lambda_{\text{sa}}^{\text{dec}}(\infty) = \max_a e^{-a} \sum_{k=1}^N \frac{a^k}{(k-1)!}. \quad (23)$$

The above are direct consequences of applying (12). Note that with the decorrelator, the maximum asymptotic throughput of slotted ALOHA can be much smaller than that of round-robin. For example, when $N = 10$, the maximum asymptotic throughput of slotted ALOHA with the decorrelator is 5.831, which is achieved at $a = 7.297$.

Remark 2: While no straightforward closed-form expressions for maximum asymptotic throughput are available for the matched filter and the linear MMSE detector, some qualitative results are possible. For round-robin, comparing (9), (12) and (14) reveals

- 1) $\Lambda_{\text{rr}}^{\text{mmse}}(\infty) \geq \Lambda_{\text{rr}}^{\text{mf}}(\infty)$, with the equality held when $N = 1$.
- 2) $\Lambda_{\text{rr}}^{\text{mmse}}(\infty) \geq \Lambda_{\text{rr}}^{\text{dec}}(\infty)$; the equality holds if and only if the throughput of the linear MMSE with $m = N + 1$ is smaller than with $m = N$, i.e.,

$$(N + 1) \left[1 - I \left(\frac{\beta}{1 + \beta}; N, 1 \right) \right] \leq N,$$

which yields

$$\beta \geq \frac{1}{(N + 1)^{1/N} - 1}.$$

In other words, the linear MMSE detector can support a throughput larger than the number of receive antennas N (and surpass the decorrelator) if and only if $\beta < \frac{1}{(N+1)^{1/N} - 1}$. Note

that the right-hand-side of the above inequality is a strictly increasing function of N , going from 1 to $+\infty$.

- 3) The relative performance of the decorrelator and the matched filter depends on β . It can be shown that when $\beta \geq 1$, $\Lambda_{\text{rr}}^{\text{dec}}(\infty) \geq \Lambda_{\text{rr}}^{\text{mf}}(\infty)$.

Remark 3: As for slotted ALOHA, since we have $q^{\text{mmse}}(m, \infty) \geq \max\{q^{\text{mf}}(m, \infty), q^{\text{dec}}(m, \infty)\}$ for all m , the maximum asymptotic throughput with the linear MMSE is always the best, while it is not immediate whether the matched filter or the decorrelator is the worst.

C. Throughput-Constrained Energy Minimization

In this section we study the optimization to achieve the greatest energy efficiency, i.e., to minimize the effective energy. In particular, we study the minimization of the effective energy subject to a throughput constraint $\lambda \geq \Delta$. There are two reasons for doing this. First, it is only fair to compare the energy efficiency of different MAC schemes if they achieve the same throughput. Second and more importantly, in a practical sensor network, there is usually a minimum throughput constraint, which may arise from a QoS demand from the end user, or from a mild delay constraint to ensure the stability of the network. As discussed in Section IV.B, the maximum asymptotic throughput is the upper limit on the throughput supportable by each MAC scheme with a given linear detector, so the given throughput constraint must not exceed this limit, otherwise it cannot be met. Comparing (16) and (19), we observe that $\sigma^2 T/G$ is a common factor and is fixed. Therefore to minimize E_e it suffices to find

$$\min_{a, \rho} \frac{a\rho}{\lambda(a, \rho)}, \quad (24)$$

subject to

$$\lambda(a, \rho) \geq \Delta. \quad (25)$$

In the following we briefly describe both single-parameter optimization as well as joint optimization.

1) *Fixed ρ :* For a fixed ρ , the throughput constraint Δ can be met if and only if $\Lambda(\rho) \doteq \max_a \lambda(a, \rho)$, the maximum throughput given ρ , satisfies $\Lambda(\rho) \geq \Delta$. When ρ is fixed, for each MAC scheme, the values of a that satisfy $\lambda(a, \rho) \geq \Delta$ form a closed interval (of reals or integers). Since $\Pr[\text{succ}]$ decreases with a , the effective energy is minimized by the minimum a

with which the throughput constraint is satisfied, i.e.,

$$a_{\text{opt}}(\rho) = \min\{a \mid \lambda(a, \rho) \geq \Delta\}. \quad (26)$$

2) *Fixed a*: When a is fixed, the throughput constraint Δ can be met if and only if $\lambda(a, \infty) \doteq \lim_{\rho \rightarrow \infty} \lambda(a, \rho)$, the maximum throughput given a , satisfies $\lambda(a, \infty) \geq \Delta$. Since the throughput is a monotone increasing function of ρ , we can find the smallest ρ that meets the throughput constraint, which is denoted by $\rho_{\min}(a) = \min\{\rho \mid \lambda(a, \rho) \geq \Delta\}$. Thus the minimum effective energy for fixed a is given by

$$E_{e,\min}(a) = \min_{\rho \geq \rho_{\min}(a)} \frac{a\rho}{\lambda(a, \rho)}. \quad (27)$$

3) *Joint Optimization*: If we can jointly optimize a and ρ and there is no power constraint, the throughput constraint Δ can be met as long as the maximum asymptotic throughput $\Lambda(\infty) \geq \Delta$. The joint optimization can be proceeded in two steps: first, find the minimum effective energy when a is fixed, as described above; then find the global minimum across all a . This is characterized by the following proposition.

Proposition 4.2: For a given throughput constraint Δ , if $\Delta \leq \Lambda(\infty)$, the minimum effective energy jointly optimized over a and ρ is given by

$$E_{e,\min} = \min_a E_{e,\min}(a) = \min_a \min_{\rho \geq \rho_{\min}(a)} \frac{a\rho}{\lambda(a, \rho)}, \quad (28)$$

while if $\Delta > \Lambda(\infty)$, the throughput constraint cannot be met.

V. NUMERICAL RESULTS AND DISCUSSIONS

In this section we present the numerical results and draw some observations on the comparative performance of different MAC schemes, as well as on the comparative performance of different linear detectors.

A. Maximum Throughput

Example 1 (Comparison of detectors; Joint Optimization): In Fig. 1 we plot the maximum asymptotic throughput (result of joint optimization) of round-robin with three linear detectors when $\beta = 1$ and $\beta = 3$. Note that the two curves for the decorrelator coincide. When $\beta = 1$, the maximum asymptotic throughput of the linear MMSE detector exceeds that of the decorrelator (which is N) for all values of N except $N = 1$, since $\frac{1}{(N+1)^{1/N-1}} > 1$ for all $N > 1$. When

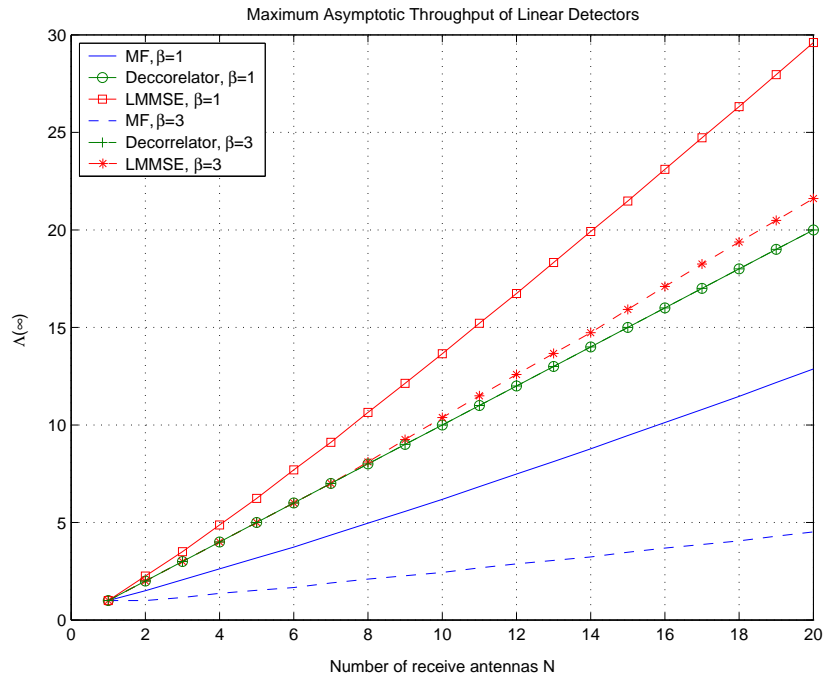


Fig. 1. Maximum asymptotic throughput of round-robin with different linear detectors

$\beta = 3$, the maximum asymptotic throughput of the linear MMSE detector exceeds that of the decorrelator when $N \geq 8$, with which $\frac{1}{(N+1)^{1/N-1}} > 3$. As β gets larger, it requires a larger N for the linear MMSE detector to surpass the decorrelator in terms of the maximum asymptotic throughput.

Example 2 (Comparison of MAC schemes and detectors; Joint Optimization): Fig. 2 shows the maximum asymptotic throughput of round-robin and slotted ALOHA with three linear detectors when $\beta = 1$. Note that the relative performance loss of slotted ALOHA with respect to round-robin is much larger with the decorrelator than with the matched filter and the linear MMSE detector. When N is small, the matched filter outperforms the decorrelator for slotted ALOHA, and when N is large, the opposite is true. For both MAC schemes the linear MMSE detector assumes great superiority, and can achieve a maximum asymptotic throughput greater than N with the linear MMSE detector when $\beta = 1$.

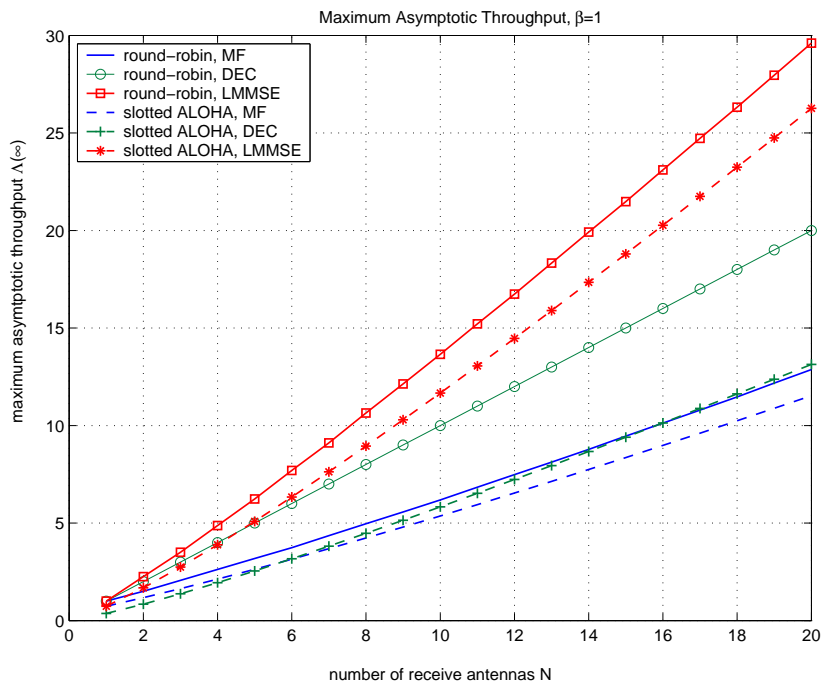


Fig. 2. Maximum asymptotic throughput of round-robin and slotted ALOHA with different linear detectors, $\beta = 1$

B. Minimum Effective Energy with Throughput Constraint

In the following we present the results of throughput-constrained energy minimization described in Section IV.C. We show the results of optimization with fixed a and joint optimization. For all simulations in this section we use the following values: $N = 10$, $\beta = 1$ and $\sigma^2 T/G = 1$ (scaling factor of E_e).

Example 3 (Comparison of MAC schemes; Fixed a): Assume that the decorrelator is used, Fig. 3 plots the minimum effective energy of three MAC schemes with the throughput constraint $\Delta = 5$ when a is fixed. Note that the throughput constraint implies that $m \geq 5$ for round-robin, and $5.21 \leq a \leq 9.43$ for slotted ALOHA. We observe that except for $m = 5$, (where the minimum effective energy of round-robin goes to infinity and is not shown in the figure), round-robin is much more energy-efficient than slotted ALOHA for the same value of a .

Example 4 (Comparison of MAC schemes; Joint optimization): Assume that the decorrelator is used, when $\Delta = 5$, Fig. 3 reveals that the minimum effective energy is achieved at $m = 6$ for round-robin, and at about $a = 6.2$ for slotted ALOHA. The minimum effective energy

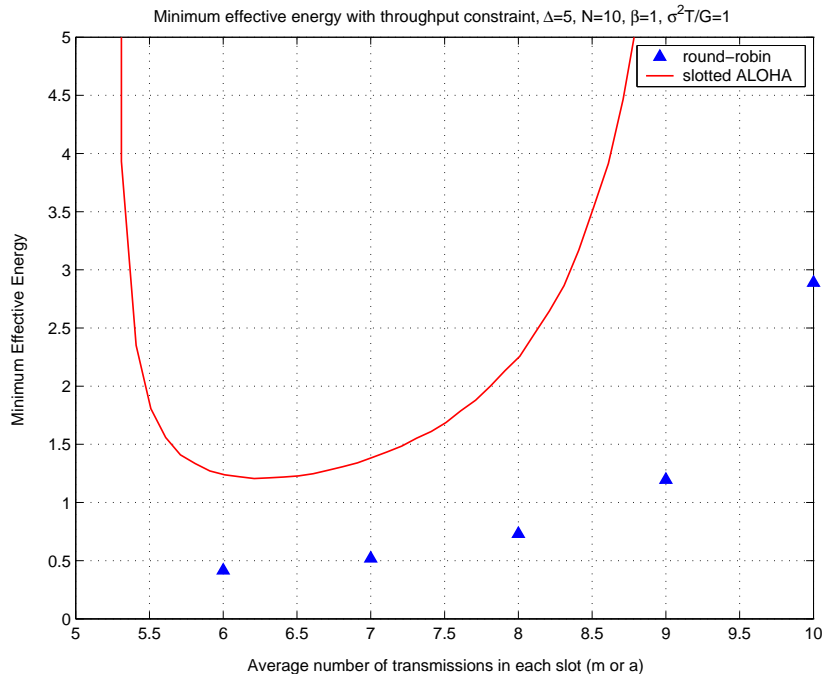


Fig. 3. Minimum effective energy with throughput constraint for different MAC schemes with the decorrelator (fixed m or a), $\Delta = 5$, $N = 10$, $\beta = 1$, $\sigma^2 T/G = 1$

corresponding to different throughput constraints obtained through jointly optimizing a and ρ is shown in Fig. 4, and the corresponding optimal a is shown in Fig. 5. Note that the largest throughput achievable by round-robin is $\Lambda(\infty) = N = 10$, and that of slotted ALOHA is 5.831. The minimum effective energy curve for round-robin is not smooth at values of m where a jump in the optimal group size m occurs. For slotted ALOHA, the optimal a is a smooth function of Δ , and so is the minimum effective energy. It can be seen from Fig. 4 that the minimum effective energy increases rapidly as Δ approaches the maximum asymptotic throughput for each MAC scheme: the minimum effective energy approaches infinity for slotted ALOHA and round-robin respectively as $\Delta \rightarrow 5.831$ and as $\Delta \rightarrow 10$. When Δ is relatively small (e.g., $\Delta \leq 3$), slotted ALOHA does not incur much extra energy expenditure than round-robin. As Δ increases, the energy saving by round-robin relative to slotted ALOHA becomes increasingly larger, and round-robin can support a throughput that cannot be achieved by slotted-ALOHA.

Example 5 (Comparison of linear detectors; Joint optimization): The throughput-constrained minimum effective energy for round-robin with various linear detectors is shown in Fig. 6.

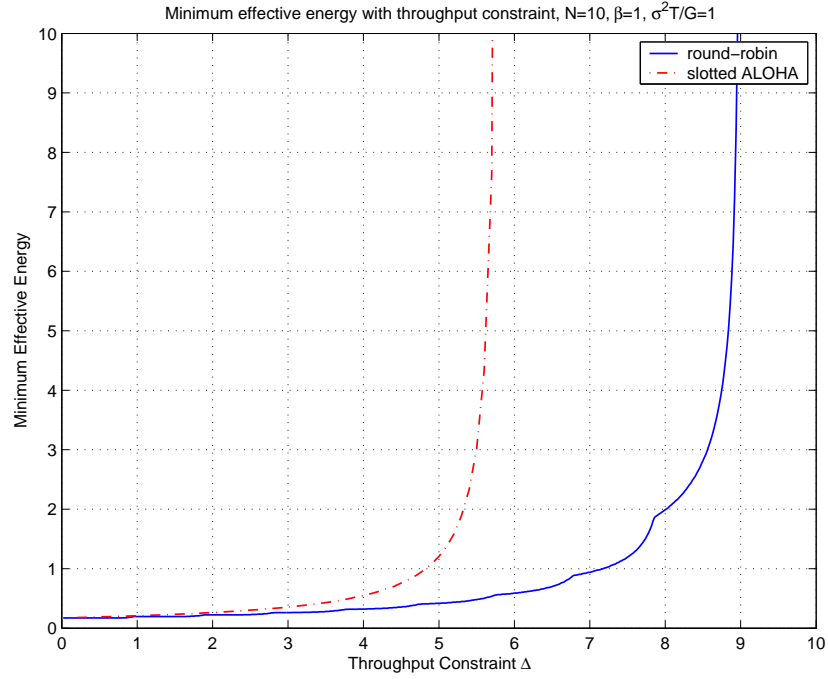


Fig. 4. Minimum effective energy with throughput constraint for different MAC schemes with the decorrelator (joint optimization), $N = 10, \beta = 1, \sigma^2 T/G = 1$

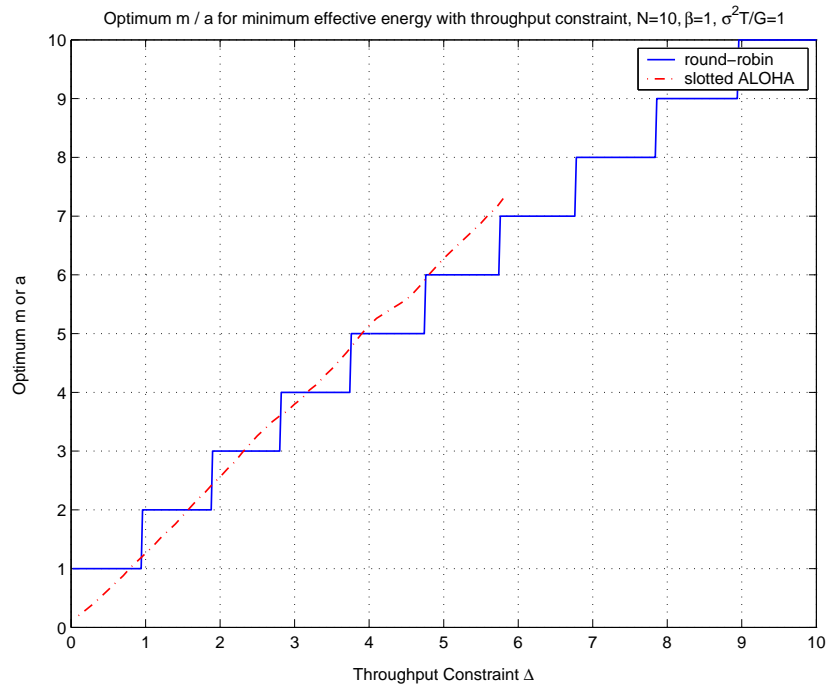


Fig. 5. Optimal m or a for minimum effective energy with throughput constraint for different MAC schemes with the decorrelator (joint optimization), $N = 10, \beta = 1, \sigma^2 T/G = 1$

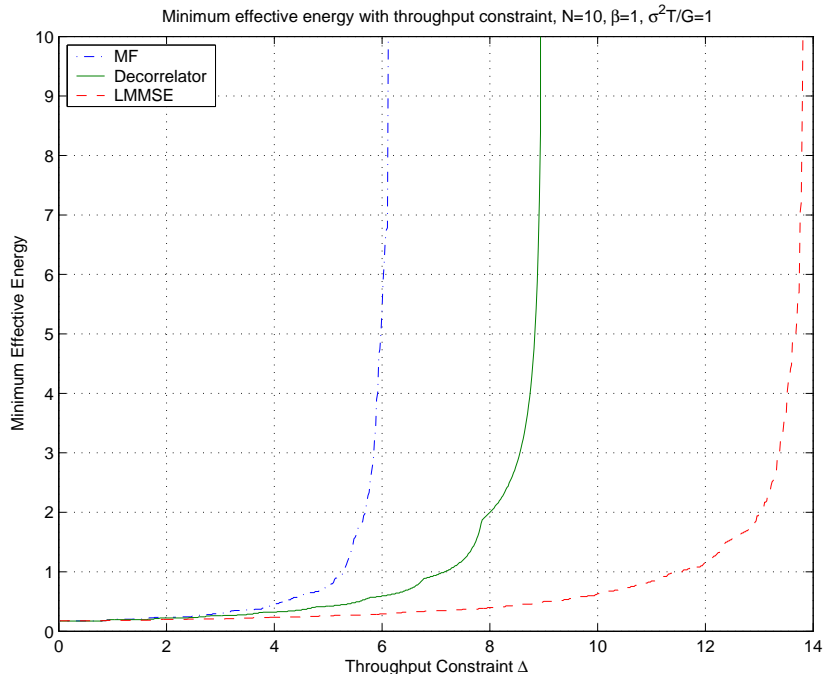


Fig. 6. Minimum effective energy with throughput constraint for round-robin with different linear detectors (joint optimization), $N = 10$, $\beta = 1$, $\sigma^2 T/G = 1$

When $N = 10$, the maximum asymptotic throughput of round-robin with the matched filter, the decorrelator and the linear MMSE detector are about 6.4, 10 and 13.8 respectively (c.f. Fig. 1). Again, it can be seen that the minimum effective energy approaches infinity as the throughput constraint approaches the maximum asymptotic throughput. When Δ is small, we can use any one of the three detectors, but with different energy expenditures. As Δ gets larger, we are left with fewer choices of the detector that can be used. The linear MMSE detector is certainly favorable in all scenarios.

VI. MULTIUSER SCHEDULING UNDER SHADOW FADING

With the assumption of independent fading across the space, multiuser diversity can be explored in a multiuser environment to achieve a scheduling gain for delay-tolerant applications. It has been shown that in a single-antenna system, the information capacity is maximized by the so-called “opportunistic transmission”, i.e., allowing only the user with the best channel to transmit in every slot [28]. Multiuser scheduling for systems with spatial diversity has been

studied in [22]–[25], and all these works aim to maximize the information capacity. Consider a similar setup as round-robin, i.e., sensors form groups of size m , the *optimal scheduler* under the multipacket reception model should maximize the throughput in terms of the number of successfully received packets in each slot. That is, in each slot, the optimal scheduler selects the group with the highest number of sensors that meet the SIR threshold. Although such an optimal scheduler is theoretically appealing, its realization requires the receiver’s knowledge of the spatial signatures of all sensors at the beginning of each slot, which is infeasible when the number of sensors is large.

Another verified problem with multiuser scheduling for a system described in Section II is that, under pure Rayleigh fading, multiuser scheduling has a vanishing relative scheduling gain as m and N increases (indicating a tradeoff between multiple antennas and multiuser diversity) [25]. While shadow fading generally increases the dynamism of individual link quantity, which leads to larger outage probability and is unfavorable to real-time applications, it can actually enhance the scheduling gain in a multiuser environment for delay-tolerant applications [25]. By slightly modifying our system model, we can investigate the multiuser scheduling gain that is realizable under the shadow fading.

We assume that the sensors in each group are adjacent to each other such that they experience the same shadow fading while sensors in different groups experience independent identically-distributed shadow fading. In each slot, the scheduler selects the group with the highest shadowing coefficient. Although this scheduler is not optimal in terms of throughput, it only requires about $1/Nm$ amount of channel knowledge compared to the optimal scheduler. Ideally, the receiver is a mobile agent which moves at the end of each slot to induce a dynamic environment such that all groups have similar chances to enjoy the best channel in the long run. Fairness can be further guaranteed by employing other methods, such as those in [29] and [30].

Denote the channel gain of the k th ($k = 1, \dots, K$) group by G_k , then for the k th group the system model in (1) is modified as

$$\mathbf{y} = \sqrt{G_k} \sum_{i=1}^m \mathbf{h}_i x_i + \mathbf{n}. \quad (29)$$

G_k is modeled as log-normal distributed, which has area mean $E[G_k] = G = G_L(\text{dB})$, and decibel spread $\sigma_L(\text{dB})$. The average SNR is given by $\rho = \frac{PG}{\sigma^2}$. Denote $G_k = e^{z_k}$, then $z_k \sim \mathcal{N}(\kappa G_L, (\kappa \sigma_L)^2)$ is a Gaussian variable, where $\kappa = \ln 10/10$.

Lemma 6.1 [31]: If Z_1, \dots, Z_K are i.i.d. Gaussian with mean μ and variance σ^2 , as $K \rightarrow \infty$,

$$\max_{1 \leq k \leq K} Z_k \rightarrow \mu + \sigma\sqrt{2 \ln K}. \quad (30)$$

Applying the lemma to z_k as defined above, we have $\max z_k \rightarrow \kappa G_L + \kappa \sigma_L \sqrt{2 \ln K}$ (dB), or $\max G_k \rightarrow G \cdot e^{\kappa \sigma_L \sqrt{2 \ln K}}$. Denote the individual SNR $\rho_k = \frac{P G_k}{\sigma^2}$, we then have $\max \rho_k \rightarrow \frac{P G}{\sigma^2} \cdot e^{\kappa \sigma_L \sqrt{2 \ln K}} \doteq \xi \rho$, where $\xi = e^{\kappa \sigma_L \sqrt{2 \ln K}}$ roughly characterizes the scheduling gain in terms of the improvement of SNR. The throughput and the effective energy of the scheduling algorithm respectively converge to

$$\lambda_{\text{sch}}(m, \rho) = m q(m, \xi \rho), \quad (31)$$

and

$$E_{\text{e,sch}}(m, \rho) = \frac{\rho \sigma^2 T / G}{q(m, \xi \rho)}. \quad (32)$$

In comparison, the throughput and effective energy of the same system via using the round-robin approach are given by

$$\lambda_{\text{rr}}(m, \rho) = E_{\rho_k} [m q(m, \rho_k)] = m \int_{-\infty}^{+\infty} q(m, e^z) \frac{e^{-(\ln z - \ln \rho)^2 / 2(\kappa \sigma_L)^2}}{z \sqrt{2\pi \kappa \sigma_L}} dz \doteq m \overline{q(m, \rho)}. \quad (33)$$

and

$$E_{\text{e,rr}}(m, \rho) = \frac{\rho \sigma^2 T / G}{\overline{q(m, \rho)}}. \quad (34)$$

The throughput of multiuser scheduling and round-robin in shadow fading, both with the decorrelator, are depicted in Fig. 7, where $N = 10, n = 1000, \sigma_L = 8\text{dB}, \beta = 1$, and two SNR values, -10dB and 0dB are shown. The throughput of round-robin without shadowing (i.e., pure Rayleigh fading) are also plotted for comparison. We observe that even for round-robin, shadowing is beneficial when the SNR is low, while the opposite is true when SNR is high: shadowing degrades the throughput. This can be readily explained by Jensen's inequality by observing the property of the $q(m, \rho)$ function: for all three detectors, it can be shown that the $q(m, \rho)$ function is convex in the low SNR range and is concave in the high SNR range, and approaches $q(m, \infty)$ as $\rho \rightarrow \infty$ (see (9), (12) and (14)). Meanwhile, the throughput of multiuser scheduling is almost invariant of the SNR, and is roughly equal to the number of transmissions. This means that despite of the average SNR, the group of the best channel has an effective SNR with which the success probability is 1. This demonstrates that multiuser scheduling is most useful when the SNR is low, which is of particular significance for sensor networks.

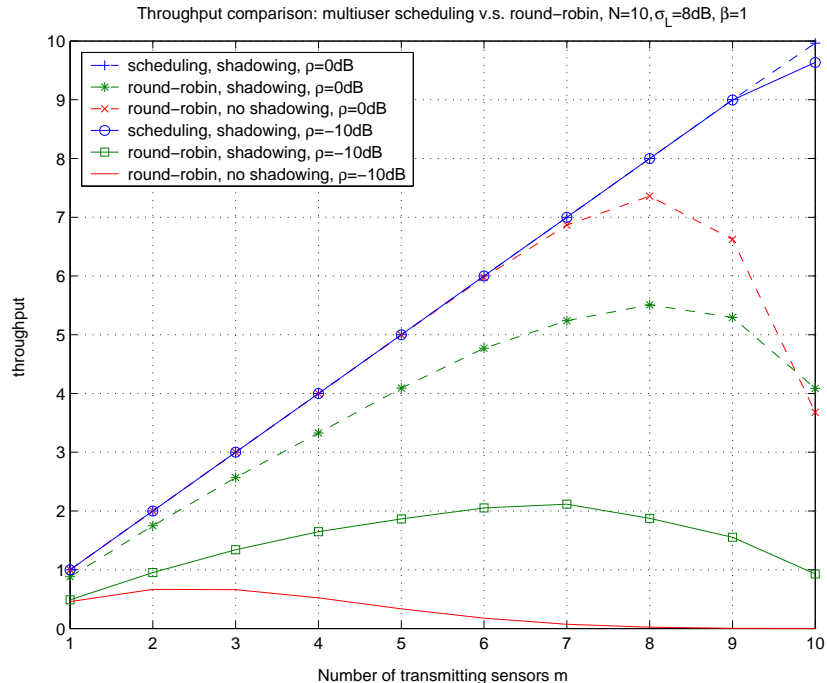


Fig. 7. Throughput comparison: multiuser scheduling v.s. round-robin (with the decorrelator), $N = 10$, $n = 1000$, $\sigma_L = 8\text{dB}$, $\beta = 1$

It is not difficult to show from (31) that the multiuser scheduling algorithm has the same maximum asymptotic throughput as round-robin. However, the fact that $q(m, \xi\rho)$ can be made virtually 1 for a modest ρ when the number of sensors is large implies that there is no loss in the energy consumption, and that the minimum effective energy remains low for all throughput constraints $\Delta < \Lambda(\infty)$.

VII. CONCLUSIONS

In this paper we have presented a detailed investigation of two important aspects in the sensor network design, the throughput and the energy efficiency, which are typically two inconsistent measures. We have considered the uplink reachback problem with simultaneous transmissions and multiple receive antennas. Simultaneous transmissions are favored for dramatically increased throughput and supported by the advanced signal processing exploited in the physical layer. We consider both coordinated and random medium access control schemes, represented respectively by round-robin and slotted ALOHA. We measure the energy efficiency with the effective energy,

defined as the average energy consumption for each successfully transmitted packet. We optimize the average number of transmissions per slot a and the transmission power per sensor node, to meet two objectives: throughput maximization, and throughput-constrained effective energy minimization. There are interesting connections between these two optimization problems. In particular, the maximum asymptotic throughput as the SNR goes to infinity defines the upper limit on the throughput constraint that can be achieved.

Under the assumption of Rayleigh flat-fading channel, we show that slotted ALOHA suffers from the greatest performance loss when paired with the decorrelator. While slotted ALOHA has similar minimum effective energy as round-robin for small throughput-constraint, it soon turns energy-inefficient as throughput-constraint increases. For both MAC schemes, the linear MMSE detector significantly outperforms the decorrelator and the matched filter in both the throughput and the energy efficiency. Finally we consider the shadowing effect on the system performance and show that multiuser scheduling greatly boosts the throughput in low SNR region and hence is of particular significance for sensor network applications.

APPENDIX I

PROOF OF LEMMA 3.1

For the matched filter, when $m = 1$,

$$\text{SIR}_i = \rho \|\mathbf{h}_i\|^2,$$

where $\|\mathbf{h}_i\|^2 \sim \chi_{2N}^2$. Thus

$$\Pr[\text{SIR}_i \geq \beta] = \Pr\left[\|\mathbf{h}_i\|^2 \geq \frac{\beta}{\rho}\right] = 1 - \Gamma\left(\frac{\beta}{\rho}, N\right),$$

where $\Gamma(a, x)$ is the regularized gamma function given by $\Gamma(a, x) = \int_0^x t^{a-1} e^{-t} dt / \int_0^\infty t^{a-1} e^{-t} dt$.

When $m > 1$, we can write the SIR in (7) as

$$\text{SIR}_i = \frac{\|\mathbf{h}_i\|^2}{\frac{1}{\rho} + \frac{\mathbf{h}_i^\dagger (\mathbf{H}_i \mathbf{H}_i^\dagger) \mathbf{h}_i}{\|\mathbf{h}_i\|^2}},$$

where \mathbf{H}_i denotes the matrix obtained by deleting the i -th column of \mathbf{H} . $\mathbf{H}_i \mathbf{H}_i^\dagger$ has a complex central Wishart distribution with $m - 1$ degrees of freedom and covariance matrix \mathbf{I}_{m-1} , denoted as $\mathbf{H}_i \mathbf{H}_i^\dagger \in CW_N(m - 1, \mathbf{I}_{m-1})$. Since \mathbf{h}_i and \mathbf{H}_i are independent, according to Theorem 3.2.8

in [32] we have

$$Y \doteq \frac{\mathbf{h}_i^\dagger (\mathbf{H}_i \mathbf{H}_i^\dagger) \mathbf{h}_i}{\|\mathbf{h}_i\|^2} \sim \chi_{2(m-1)}^2,$$

and Y is independent of \mathbf{h}_i . Denote $X \doteq \|\mathbf{h}_i\|^2 \sim \chi_{2N}^2$. Therefore, the probability of success is

$$\Pr [\text{SIR}_i \geq \beta] = \Pr \left[X \geq \beta \left(Y + \frac{1}{\rho} \right) \right] = \frac{1}{(m-2)!} \int_0^\infty [1 - \Gamma(\beta y + \beta/\rho), N] y^{m-2} e^{-y} dy.$$

In summary,

$$q^{\text{mf}}(m, \rho) = \begin{cases} 1 - \Gamma(\beta/\rho, N), & m = 1, \\ \frac{1}{(m-2)!} \int_0^\infty [1 - \Gamma(\beta y + \beta/\rho), N] y^{m-2} e^{-y} dy, & m > 1. \end{cases}$$

As $\rho \rightarrow \infty$, when $m > 1$, we have

$$\text{SIR}_i = \frac{X}{Y} = \frac{N}{m-1} \frac{X/2N}{Y/2(m-1)} \doteq \frac{N}{m-1} F,$$

where $F = \frac{X/2N}{Y/2(m-1)}$ has an $F_{2N, 2(m-1)}$ distribution. Therefore,

$$\Pr [\text{SIR}_i \geq \beta] = \Pr \left[F \geq \beta \frac{m-1}{N} \right] = 1 - I\left(\frac{\beta}{1+\beta}; N, m-1\right),$$

where $I(x; a, b)$ is the regularized beta function, given by $I(x; a, b) = \frac{\int_0^x t^{a-1}(1-t)^{b-1} dt}{\int_0^1 t^{a-1}(1-t)^{b-1} dt}$. It is obvious that when $\rho \rightarrow \infty$, $\Pr [\text{SIR}_i \geq \beta] = 1$ for $m = 1$, thus we have

$$q^{\text{mf}}(m, \infty) = \begin{cases} 1, & m = 1, \\ 1 - I\left(\frac{\beta}{1+\beta}; N, m-1\right), & m > 1. \end{cases}$$

APPENDIX II

PROOF OF LEMMA 3.2

Denote the $m \times m$ matrix $\mathbf{Z} \doteq \mathbf{H}^\dagger \mathbf{H}$, then \mathbf{Z} has a complex central Wishart distribution, i.e., $\mathbf{Z} \in CW_m(N, \mathbf{I}_N)$. It is known that when $m \leq N$, the determinant of \mathbf{Z} is distributed as $\prod_{i=1}^m \chi_{2(N-i+1)}^2$, and when $m > N$, \mathbf{Z} is singular [32]. Therefore we have when $m \leq N$,

$$z_i \doteq \frac{1}{(\mathbf{Z}^{-1})_{ii}} = \frac{\det(\mathbf{Z})}{\det(\mathbf{Z}_{[i]})} = \det(\mathbf{Z}_{[i]}^{\text{sc}}),$$

where $\mathbf{Z}_{[i]}$ denotes the matrix obtained by striking out the i -th row and the i -th column of \mathbf{Z} , and $\mathbf{Z}_{[i]}^{\text{sc}}$ denotes the Schur-complement of $\mathbf{Z}_{[i]}$, which is also complex Wishart distributed, i.e., $\mathbf{Z}_{[i]}^{\text{sc}} \in CW_1(N - m + 1, \mathbf{I}_{N-m+1})$. Therefore, $z_i = \det(\mathbf{Z}_{[i]}^{\text{sc}}) \sim \chi_{2(N-m+1)}^2$. We get for the decorrelating detector, when $m \leq N$,

$$\Pr [\text{SIR}_i \geq \beta] = \Pr \left[z_i \geq \frac{\beta}{\rho} \right] = 1 - \Gamma\left(\frac{\beta}{\rho}, N - m + 1\right),$$

while when $m > N$, since $\text{SIR}_i = 0$, $\Pr[\text{SIR}_i \geq \beta] = 0$. In summary,

$$q^{\text{dec}}(m, \rho) = \begin{cases} 1 - \Gamma(\beta/\rho, N - m + 1), & m \leq N, \\ 0, & m > N. \end{cases}$$

APPENDIX III

PROOF OF LEMMA 3.3

For the linear MMSE detector, when $m < N$, consider the limiting SIR as $\rho \rightarrow \infty$

$$\lim_{\rho \rightarrow \infty} \text{SIR}_i = \lim_{\rho \rightarrow \infty} \mathbf{h}_i^\dagger \left(\mathbf{H}_i \mathbf{H}_i^\dagger + \frac{1}{\rho} \mathbf{I} \right)^{-1} \mathbf{h}_i = \lim_{\rho \rightarrow \infty} \rho \mathbf{h}_i^\dagger \left(\rho \mathbf{H}_i \mathbf{H}_i^\dagger + \mathbf{I} \right)^{-1} \mathbf{h}_i.$$

Denote the spectral decomposition of matrix $\mathbf{H}_i \mathbf{H}_i^\dagger = \mathbf{U} \mathbf{D} \mathbf{U}^\dagger$, where \mathbf{D} is the matrix containing the eigenvalues of $\mathbf{H}_i \mathbf{H}_i^\dagger$ in decreasing order, and \mathbf{U} is the unitary matrix containing the eigenvectors of $\mathbf{H}_i \mathbf{H}_i^\dagger$. Putting in the above and evaluating the limit, we get

$$\lim_{\rho \rightarrow \infty} \text{SIR}_i = \rho \mathbf{h}_i^\dagger \mathbf{U} \mathbf{Q} \mathbf{U}^\dagger \mathbf{h}_i = \rho \mathbf{v}_i^\dagger \mathbf{Q} \mathbf{v}_i.$$

where $\mathbf{Q} = \text{diag}(0, \dots, 0, 1, \dots, 1)$, and the number of 1's is the number of zero eigenvalues of $\mathbf{H}_i \mathbf{H}_i^\dagger$, which is $N - m + 1$, and $\mathbf{v} = \mathbf{U}^\dagger \mathbf{h}_i$. Since \mathbf{h}_i is circularly symmetric complex Gaussian, \mathbf{v} has the same distribution as \mathbf{h}_i . Therefore, $\lim_{\rho \rightarrow \infty} \text{SIR}_i = \rho \sum_{i=1}^{N-m+1} \|\mathbf{v}_i\|^2 \sim \rho \chi_{2(N-m+1)}^2$, which is the same as the decorrelator. Thus $q(m, \infty) = \lim_{\rho \rightarrow \infty} 1 - \Gamma\left(\frac{\beta}{\rho}, N - m + 1\right) = 1$.

When $m > N$, $\mathbf{H}_i \mathbf{H}_i^\dagger$ is invertible, so as $\rho \rightarrow \infty$,

$$\text{SIR}_i \rightarrow \mathbf{h}_i^\dagger \left(\mathbf{H}_i \mathbf{H}_i^\dagger \right)^{-1} \mathbf{h}_i.$$

Since \mathbf{h}_i and \mathbf{H}_i are independent, and $\mathbf{H}_i \mathbf{H}_i^\dagger \in CW_N(m-1, \mathbf{I}_{m-1})$, using Theorem 3.2.12 in [32] we obtain

$$Z \doteq \frac{\|\mathbf{h}_i\|^2}{\mathbf{h}_i^\dagger \left(\mathbf{H}_i \mathbf{H}_i^\dagger \right)^{-1} \mathbf{h}_i} \sim \chi_{2(m-N)}^2,$$

and Z is independent of \mathbf{h}_i . Denoting $X \doteq \|\mathbf{h}_i\|^2$, we get

$$\mathbf{h}_i^\dagger \left(\mathbf{H}_i \mathbf{H}_i^\dagger \right)^{-1} \mathbf{h}_i = \frac{X}{Z} = \frac{N}{m-N} \frac{X/2N}{Z/2(m-N)} \doteq \frac{N}{m-N} F,$$

where $F = \frac{X/2N}{Z/2(m-N)}$ has an $F_{2N, 2(m-N)}$ distribution. Therefore,

$$\Pr[\text{SIR}_i \geq \beta] = \Pr\left[F \geq \beta \frac{m-N}{N}\right] = 1 - I\left(\frac{\beta}{1+\beta}; N, m-N\right).$$

In summary,

$$q^{\text{mmse}}(m, \infty) = \begin{cases} 1, & m \leq N, \\ 1 - I\left(\frac{\beta}{1+\beta}; N, m-N\right), & m > N. \end{cases}$$

REFERENCES

- [1] I. F. Akyidiz, Y. S. W. Su, and E. Cayirci, "A survey on sensor networks," *IEEE Commun. Magazine*, vol. 9, no. 4, pp. 102–114, Aug. 2002.
- [2] A. J. Goldsmith and S. B. Wicker, "Design challenges for energy-constrained ad hoc wireless networks," *IEEE Commun. Magazine*, vol. 9, no. 4, pp. 8–27, Aug. 2002.
- [3] E. Shih, S. Cho, N. Ickes, R. Min, A. Sinha, A. Wang, and A. Chandrakasan, "Physical layer driven protocol and algorithm design for energy-efficient wireless sensor networks," in *Proc. International Conference on Mobile Computing and Networking*, Rome, Italy, 2001.
- [4] A. Dana and B. Hassibi, "On the power-efficiency of sensory and ad-hoc wireless networks," submitted to *IEEE Transactions on Information Theory*.
- [5] S. Cui and A. J. Goldsmith, "Energy-constrained modulation optimization," *IEEE Tran. Wireless Commun.*, to appear.
- [6] J. Chou, D. Petrovic, and K. Ramachandran, "A distributed and adaptive signal processing approach to reducing energy consumption in sensor networks," in *Proc. IEEE INFOCOM 2003*, San Francisco, CA, 2003.
- [7] S. Cui, R. Madan, A. J. Goldsmith, and S. Lall, "Joint routing, mac, and link layer optimization in sensor networks with energy constraints," to appear in *ICC 2005*.
- [8] A. Ephremides, "Energy concerns in wireless networks," *IEEE Wireless Communications*, vol. 9, pp. 48–52, Aug. 2002.
- [9] L. Tong, Q. Zhao, and S. Adireddy, "Sensor networks with mobile agents," in *Proc. of IEEE Military Comm. Conf.*, Boston, MA, Oct. 2003.
- [10] L. Roberts, "ALOHA packet system with and without slots and capture," *Computer Communications Review*, vol. 5, pp. 28–42, Apr. 1975.
- [11] S. Verdú, *Multuser Detection*. Cambridge, U.K.: Cambridge University Press, 1998.
- [12] S. Ghez, S. Verdu, and S. Schwartz, "Stability properties of slotted Aloha with multipacket reception capability," *IEEE Tran. Automatic Control*, vol. 33, pp. 640–649, July 1988.
- [13] B. Hajek, A. Krishna, and R. O. Lemaire, "On the capture probability for a large number of stations," *IEEE Tran. Commun.*, vol. 45, pp. 254–260, Feb. 1997.
- [14] S. V. Hanly and D. N. C. Tse, "Resource pooling and effective bandwidths in CDMA networks with multiuser receivers and spatial diversity," *IEEE Tran. Inform Theory*, vol. 47, pp. 1328–1351, May 2001.
- [15] S. Ghez, S. Verdu, and S. Schwartz, "Optimal decentralized control in the random access multipacket channel," *IEEE Tran. Automatic Control*, vol. 34, pp. 1153–1163, Nov. 1989.
- [16] S. Adireddy and L. Tong, "Exploiting decentralized channel state information for random access," *IEEE Tran. Info. Theory*, vol. 51, pp. 537–561, Feb. 2005.
- [17] A. Chockalingam, M. Zorzi, L. B. Milstein, and P. Venkataram, "Performance of a wireless access protocol on correlated rayleigh-fading channels with capture," *IEEE Tran. Communications*, vol. 46, pp. 644–655, May 1998.
- [18] J. T.-K. Liu and A. Polydoros, "Retransmission control and fairness issue in mobile slotted ALOHA networks with fading and near-far effect," *Mobile Networks and Applications*, vol. 2, pp. 101–10, 1997.
- [19] X. Qin and R. Berry, "Exploiting multiuser diversity in wireless ALOHA networks," in *Proc. Allerton Conference on Communication, Control and Computing*, Allerton, IL, Oct. 2001.
- [20] P. Venkitasubramaniam, Q. Zhao, and L. Tong, "Sensor network with multiple mobile access points," in *Proc. Conference on Information Sciences and Systems*, Princeton, NJ, Mar. 2004.

- [21] W. Li and H. Dai, "Throughput and energy efficiency of sensor networks with multiuser receivers and spatial diversity," in *Proc. IEEE International Conference on Acoustics, Speech, and Signal Processing (ICASSP) 2005*, Philadelphia, PA, Mar. 2005.
- [22] E. Larsson, "On the combination of spatial diversity and multiuser diversity," *IEEE Communications Letters*, vol. 8, pp. 517–519, Aug. 2004.
- [23] J. Jiang, R. M. Buehrer, and W. H. Tranter, "Antenna diversity in multiuser data networks," *IEEE Tran. Commun.*, vol. 52, pp. 490–497, Mar. 2004.
- [24] D. Aktas and H. E. Gamal, "Multiuser scheduling for MIMO wireless systems," in *Proc. IEEE Vehicular Technology Conference 2003-Fall*, Orlando, FL, Oct. 2003.
- [25] B. M. Hochwald, T. L. Marzetta, and V. Tarokh, "Multiple-antenna channel hardening and its implications for rate feedback and scheduling," *IEEE Tran. Inform. Theory*, vol. 50, pp. 1893 – 1909, Sept. 2004.
- [26] X. Liu, E. K. P. Chong, and N. B. Shroff, "Opportunistic transmission scheduling with resource-sharing constraints in wireless networks," *IEEE J. Selected Areas of Communications*, vol. 19, pp. 2053–2064, Oct. 2001.
- [27] D. N. C. Tse and O. Zeitouni, "Linear multiuser receivers in random environments," *IEEE Tran. Inform Theory*, vol. 46, pp. 171–188, Jan. 2000.
- [28] R. Knopp and P. A. Humblet, "Information capacity and power control in single cell multiuser communications," in *Proc. IEEE Int. Conf. Commun. (ICC)*, Seattle, WA, 1995.
- [29] P. Viswanath, D. N. C. Tse, and R. Laroia, "Opportunistic beamforming using dumb antennas," *IEEE Tran. Inform Theory*, vol. 48, pp. 1277–1294, 2002.
- [30] M. Sharif and B. Hassibi, "Delay analysis of throughput optimal scheduling in broadcast fading channels," submitted to *IEEE Tran. Inform. Theory*.
- [31] H. A. David and H. N. Nagaraja, *Order Statistics*, 3rd ed. John Wiley & Sons, 2003.
- [32] R. J. Muirhead, *Aspects of multivariate statistical theory*. John Wiley & Sons, 1982.
- [33] B. Chen and L. Tong, "Traffic modeling and tracking for multiuser detection for random access networks," in *Proc. 2000 Intl. Conf. Acoust. Speech and Sig. Proc.*, Istanbul, Turkey, 2000.
- [34] S. Cui, A. J. Goldsmith, and A. Bahai, "Energy-efficiency of mimo and cooperative MIMO in sensor networks," *IEEE Journal on Selected Areas of Communications*, vol. 22, Aug. 2004.
- [35] L. Tong, V. Naware, and P. Venkitasubramaniam, "Signal processing in random access," *IEEE Signal Processing Magazine*, vol. 21, no. 5, pp. 29–39, Aug. 2004.